The dispersion relation and time evolution of a twisted planar ring

Abstract

In this report I study the Kirchhoff equations, which are the basis for considering elastic filaments, in the context of a twisted planar ring. I apply an arc length preserving perturbation scheme that perturbs the basis used to describe the system directly, and analyse the generated normal mode solutions up to second-order. I also consider how these modes evolve in time.

1 Introduction

Filaments, elastic rods which are far longer than the scale of their cross section, can be found in many physical systems [8, 9, 12]. One of the initial inspirations for their study was the difficulties faced laying marine telephone cables; currents forced regions of high and low tension along a cable, causing the cables to writhe and not lay straight. Work by Zajac [18], for example, began to explore this problem. Other work in this area considers initially straight rods and their evolution [11, 15]; however the twisted planar ring, a rod in a planar ring with some twist about the central axis, is also of interest but has not been examined as extensively [3, 6]. For example, there are applications in considering thermal fluctuations in DNA, [13, 14], where the modes described in this report are considered as a statistical mechanical ensemble of many DNA rings modelled as elastic rings. They have also been used considering how microscopic elastic rings (such as a bundle of F-Actin formed into a circle) can act as self-propelling motors [16].

A well established approach to studying elastic rods is to consider the Kirchhoff equations, a classically derived set of equations describing the system. In order to study these previously, much work has gone into static stability analysis, outlined in [3], and numerical modelling [10]. Static analysis is limited, as it does not explain the time evolution of the modes seen in numerical models. This report follows the work of Goriely and Tabor [3, 4, 6, 7] by expanding an arc length conserving direct basis expansion, which obtains explicit forms for the modes and details their evolution. It also lays the foundation for a nonlinear analysis such as that previously completed for straight rods [4].

In this report I will present the Kirchhoff equations under this perturbation scheme (sections 2, 3) in the specific case of the twisted planar ring (section 4). I consider the first-order solution to the problem, present the dispersion relation defining the modes, and consider the shape these modes take (section 5). I then proceed to consider their evolution in time (section 6) before finally considering how the form of these modes differs at higher order (section 7).

2   The Kirchhoff Model

The first tool that is needed to analyse a rod in space is an appropriate geometrical construction. A local, orthonormal basis is required to describe the twisting rod, call it $D = \{d_1, d_2, d_3\}$. Take a curve in space, $x(s,t)$, and initially define its tangent to be the first vector of this triad, $d_3 = x'$, where the $'$ denotes differentiation with respect to s. Thus d_1 and d_2 describe the orientation of the cross section in the tangent plane. This construction is called the director basis.

Typically in differential geometry [2], the director basis is constructed with $d_1 = d_3'$ and $d_2 = d_3 \times d_1$, a basis known as the Frenet basis. This basis is convenient when considering curves in space as its spatial evolution can be completely described by the Frenet-Serret formulas [2]. However this basis is inappropriate in this instance, as it only considers a curve, not a rod which can have twist. For a ring of twist T, and inverse radius k, define the twist density $\gamma = Tk$. An appropriate basis can be constructed by rotating the Frenet basis by angle γs about d_3. For a planar ring, the standard Frenet basis would be defined by $B = \{b_1, b_2, b_3\}$, where

$$b_1 = (\sin(ks), \cos(ks), 0)$$
$$b_2 = (0, 0, 1)$$
$$b_3 = (\cos(ks), -\sin(ks), 0).$$

A director basis $D = R(\gamma s)B$ is then created, where $R(\gamma s)$ is the relevant rotation,

$$d_1 = (\cos(\gamma s)\sin(ks), \cos(ks)\cos(\gamma s), \sin(\gamma s))$$
$$d_2 = (-\sin(\gamma s)\sin(ks), -\cos(ks)\sin(\gamma s), \cos(\gamma s)) \tag{1}$$
$$d_3 = (\cos(ks), -\sin(ks), 0).$$

The evolution of this geometry is described by the curvature and spin tensors; these are defined by $D' = KD$ and $\dot{D} = WD$ respectively, with the dot representing differentiation with respect to t. As the director basis is orthonormal, $D^T D = I$. Differentiating this identity shows

$$D^T K^T D + D^T K D = 0,$$

hence $K + K^T = 0$. Thus K and W are antisymmetric, defined by

$$K = \begin{pmatrix} 0 & \kappa_3 & -\kappa_2 \\ -\kappa_3 & 0 & \kappa_1 \\ \kappa_2 & -\kappa_1 & 0 \end{pmatrix}, \quad W = \begin{pmatrix} 0 & \omega_3 & -\omega_2 \\ -\omega_3 & 0 & \omega_1 \\ \omega_2 & -\omega_1 & 0 \end{pmatrix}.$$

This also introduces the curvature and spin vectors, $\boldsymbol{\kappa}$ and $\boldsymbol{\omega}$ respectively. These two tensors must be compatible under cross differentiation, that is $W' = \dot{K}$. This condition leads to the compatibility equation:

$$W' - \dot{K} = [W, K]. \tag{2}$$

where $[W, K]$ is the matrix commutator, $WK - KW$.

Armed with this construction for the director basis, the dynamics of the problem can be considered. All forces and moments can be expanded in the director basis, $F = \sum f_i d_i$ and $M = \sum m_i d_i$. Conservation of linear and angular momentum yields the Kirchhoff equations [3]

$$F'' = \rho A \ddot{d}_3 \tag{3}$$

$$M' + d_3 \times F = \rho I (d_1 \times \ddot{d}_1 + d_2 \times \ddot{d}_2), \tag{4}$$

where I is the moment of inertia of the circular cross section A. The constitutive equation for the moment when considering a circular cross section is given by

$$M = EI \left[(\kappa_1 - \kappa_1^\mu) d_1 + (\kappa_2 - \kappa_2^\mu) d_2 \right] + 2\mu I (\kappa_3 - \kappa_3^\mu) d_3, \tag{5}$$

where E is the Young's modulus for the material, μ is the shear modulus, and κ^μ represents the unstressed configuration. I shall consider an initially unstressed rod, for which $\kappa_i^\mu = 0$. Note that it is possible to study systems in which this is not the case, such as in the helix hand reversal exhibited in climbing plants [5].

There are a few assumptions in this analysis that need to be considered. The rod has a uniformly circular cross section; no shear deformation is allowed. Thus the moment of inertia is equal regardless of direction considered. There is also no axial extensibility, and the constitutive relation for the moment, given by Eq. (5), is assumed linear in curvature.

In order to convert these equations into a more manageable form, scaling is introduced [1]:

$$t \to t\sqrt{\frac{I\rho}{AE}} \qquad s \to s\sqrt{\frac{I}{A}} \qquad F \to FAE$$

$$M \to ME\sqrt{AI} \qquad \kappa \to \kappa\sqrt{\frac{A}{I}} \qquad \omega \to \sqrt{\frac{AE}{I\rho}}.$$

On the application of this scaling, the Kirchhoff equations become

$$\begin{aligned} F'' &= \ddot{d}_3 \\ M' + d_3 \times F &= d_1 \times \ddot{d}_1 + d_2 \times \ddot{d}_2 \\ M &= \kappa_1 d_1 + \kappa_2 d_2 + \Gamma \kappa_3 d_3. \end{aligned} \tag{6}$$

The result of this scaling is that there is now only one remaining parameter, $\Gamma = 2\mu/E$, which is a measure of the elasticity of the material. Most materials have a Γ between $2/3$ for perfectly incompressible materials and 1 for hyper-elastic materials. This is similar to Poisson's ratio, and further discussion of material elasticity can be found in [17]. Together with the compatibility equation (Eq. (2)), the scaled Kirchhoff equations in Eq. (6) form a complete description of the system.

3 Perturbation Scheme

In order to look at solutions to Eq. (6), one can either model it numerically [10], or use perturbation theory. This section details the perturbation scheme used. I follow the path set out by Goriely and Tabor [3,4,6,7] and perturb the director basis directly,

$$D = AD^{(0)} = \left(I + \epsilon A^{(1)} + \epsilon^2 A^{(2)} + ... \right) D^{(0)},$$

where $A^{(m)}$ represents the mth order perturbation of A. By requiring the director basis to remain orthonormal, it is possible to find the forms of the matrices $A^{(m)}$. Starting from the requirement that the director basis must be orthonormal, i.e. $D^T D = I$, this gives

$$\left(D^{(0)}\right)^T \left(I + \epsilon \left(A^{(1)}\right)^T + \epsilon^2 \left(A^{(2)}\right)^T + ...\right)\left(I + \epsilon A^{(1)} + \epsilon^2 A^{(2)} + ...\right) D^{(0)} = I.$$

This equation gives an expression at each order in ϵ defining the matrices A^m. To first-order in ϵ,

$$D^T \left(\left(A^{(1)}\right)^T + A^{(1)}\right) D = 0.$$

It follows that $A^{(1)}$ is an antisymmetric matrix,

$$A^{(1)} = \begin{pmatrix} 0 & \alpha_3^{(1)} & -\alpha_2^{(1)} \\ -\alpha_3^{(1)} & 0 & \alpha_1^{(1)} \\ \alpha_2^{(1)} & -\alpha_1^{(1)} & 0 \end{pmatrix}.$$

This approach is continued at higher order, for example at second-order the matrix $A^{(2)}$ must satisfy

$$\left(A^{(2)}\right)^T + A^{(2)} + \left(A^{(1)}\right)^T A^{(1)} = 0$$

In other words, it is composed of an antisymmetric part, introducing the parameters $\alpha_1^{(2)}$, $\alpha_2^{(2)}$ and $\alpha_3^{(2)}$, and a symmetric part depending upon $\boldsymbol{\alpha}^{(1)}$,

$$A^{(2)} = \begin{pmatrix} 0 & \alpha_3^{(2)} & -\alpha_2^{(2)} \\ -\alpha_3^{(2)} & 0 & \alpha_1^{(2)} \\ \alpha_2^{(2)} & -\alpha_1^{(2)} & 0 \end{pmatrix} + \frac{1}{2}\begin{pmatrix} -(\alpha_2^{(1)})^2 - (\alpha_3^{(1)})^2 & \alpha_1^{(1)}\alpha_2^{(1)} & \alpha_1^{(1)}\alpha_3^{(1)} \\ \alpha_1^{(1)}\alpha_2^{(1)} & -(\alpha_1^{(1)})^2 - (\alpha_3^{(1)})^2 & \alpha_2^{(1)}\alpha_3^{(1)} \\ \alpha_1^{(1)}\alpha_3^{(1)} & \alpha_2^{(1)}\alpha_3^{(1)} & -(\alpha_1^{(1)})^2 - (\alpha_2^{(1)})^2 \end{pmatrix}.$$

This structure is also exhibited at higher order, with $A^{(m)}$ being composed of an antisymmetric matrix—adding new parameters—and a symmetric one depending upon the lower order terms.

All terms can be expanded in terms of this expansion of the director basis. Firstly, the curvature tensor, which defines spatial derivatives $D' = KD$,

$$A'D^{(0)} + A\left(D^{(0)}\right)' = KAD^{(0)}$$

$$A' + A\left(K^{(0)}\right)' = KA$$

$$K = \left(A' + A\left(K^{(0)}\right)'\right)A^T.$$

Secondly for the spin tensor, which defines temporal derivatives $\dot{D} = WD$,

$$W = \left(A' + A\left(W^{(0)}\right)'\right)A^T.$$

And finally, for the force vector $\boldsymbol{f}$,

$$\boldsymbol{f}_i = \boldsymbol{f}_i^{(0)} + \epsilon \boldsymbol{f}_i^{(1)} + \epsilon^2 \boldsymbol{f}_i^{(2)} + \dots .$$

With all of the key quantities expanded, it is now possible to construct the Kirchhoff equations to nth order. This results in a set of equations at each order in ϵ, in terms of the six-dimensional vectors $\{\boldsymbol{\alpha}^{(n)}, \boldsymbol{f}^{(n)}\}$ and their derivatives.

4 The Planar Ring

Everything preceding this section has been generally applicable for any rod with a circular cross section, however now I shall look at the specific case of a planar ring with some axial twist—the twisted planar ring. The geometry of this ring is described by Eq. (1), with the director basis rotating in the tangent plane as s varies. Requiring continuity of this basis at $s = 2\pi/k$ requires γ/k to be an integer, forcing periodic boundary conditions. For a ring of inverse radius k and twist density γ, the curvature and force take the unperturbed forms

$$\boldsymbol{\kappa}^{(0)} = (k \sin(\gamma s), k \cos(\gamma s), \gamma)$$
$$\boldsymbol{f}^{(0)} = (\Gamma \gamma k \sin(\gamma s), \Gamma \gamma k \cos(\gamma s), 0) .$$

When these expressions are substituted into the expressions given by the perturbation expansion of the Kirchhoff equations, the resulting system contains terms depending upon s—it is non-autonomous. This is tackled by introducing a transformation, consisting of a rotation of angle γs and a reflection, described by the matrix

$$R_\gamma = \begin{pmatrix} \cos(\gamma s) & -\sin(\gamma s) & 0 \\ -\sin(\gamma s) & -\cos(\gamma s) & 0 \\ 0 & 0 & 1 \end{pmatrix} . \tag{7}$$

The application of this rotation to the director basis and the vectors $\boldsymbol{\alpha}^{(n)}$ and $\boldsymbol{f}^{(n)}$ forms an autonomous system. To first-order, in terms of the six-dimensional vector $\boldsymbol{\beta} = \boldsymbol{\beta}^{(1)} = \{R_\gamma \boldsymbol{\alpha}^{(1)}, R_\gamma \boldsymbol{f}^{(1)}\}$,

$$2\Gamma \gamma k^2 \beta_1' + \ddot{\beta}_2 + \Gamma \gamma k^3 \beta_3 - k\Gamma \gamma \beta_3'' - k^2 \beta_4 + \beta_4'' + 2k\beta_6' = 0$$
$$-\ddot{\beta}_1 + \beta_5'' = 0$$
$$\Gamma \gamma k \beta_1'' - \Gamma \gamma k^3 \beta_1 + 2\Gamma \gamma k^2 \beta_3' - 2k\beta_4' - k^2 \beta_6 + \ddot{\beta}_6 = 0$$
$$\beta_1'' - \ddot{\beta}_1 - (\Gamma - 1)k^2 \beta_1 - \Gamma \gamma \beta_2' + \Gamma k \beta_3' + \beta_5 = 0$$
$$\Gamma \gamma \beta_1' - \ddot{\beta}_2 + \beta_2'' + \Gamma \gamma k \beta_3 - \beta_4 = 0$$
$$-k\Gamma \beta_1' + \Gamma \beta_3'' - 2\ddot{\beta}_3 = 0.$$

This is an equation of the form

$$\hat{L}_0 \cdot \boldsymbol{\beta} = 0. \tag{8}$$

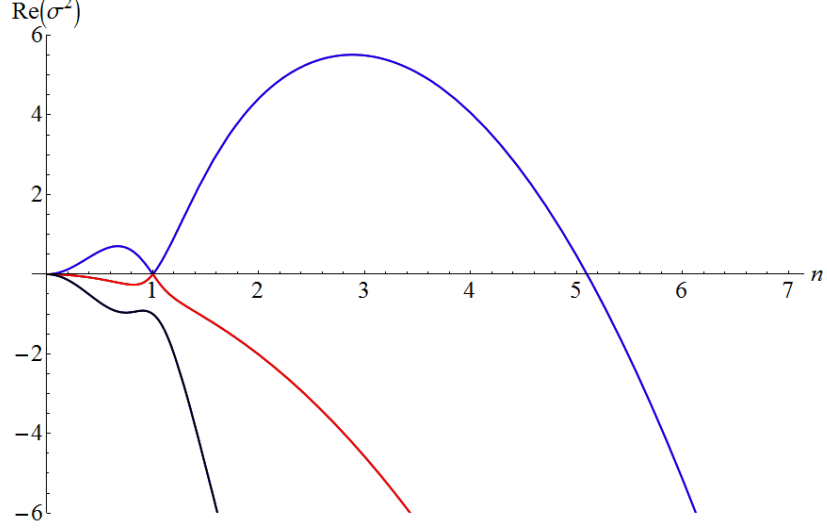This transformation can be carried out at higher order, generating the equation

5

Figure 1: The dispersion relation between $\Re(\sigma^2)$ and n (as defined by the mode solutions $e^{ikns+\sigma t}$), plotted for $k = 1$, $\Gamma = 1$ and $\gamma = 5$. The three possible curves for modes to lie on are shown here, but they also extend symmetrically into $n < 0$. The blue curve represents the possible unstable modes—with $n = 2, 3, 4, 5$ being possible unstable modes for the system. Values of n greater than the critical value, here $n_c \approx 5.10$, have no possible unstable modes. The red and black curves show stable branches of the dispersion relation.

$$\hat{L}_0 \cdot \boldsymbol{\beta}^{(n)} = H_n[\boldsymbol{\beta}^{(1)}, \boldsymbol{\beta}^{(2)}, \dots, \boldsymbol{\beta}^{(n-1)}], \tag{9}$$

where H_n is a function of $\boldsymbol{\beta}^{(m)}$s and their derivatives up to order $n - 1$. This system is solvable, and in the next section I begin to explore the first-order solution.

5   The Dispersion Relation and Normal Mode Solutions

Consider normal mode solutions to Eq. (8) of the form $\boldsymbol{\beta} = \boldsymbol{x}e^{\sigma t + ikns}$; the periodic boundary conditions require n to be an integer. Substituting this solution into Eq. (8) yields an equation of the form $M \cdot \boldsymbol{x} = 0$, with

$$M = \begin{pmatrix} 2i\Gamma\gamma k^3 n & \sigma^2 & \Gamma\gamma k^3(1+n^2) & 0 & 2ik^2 n \\ -\sigma^2 & 0 & 0 & 0 & -k^2 n^2 & 0 \\ -\Gamma\gamma k^3(1+n^2) & 0 & 2i\Gamma\gamma k^3 n & -2ik^2 n & 0 & -k^2(1+n^2) \\ -\sigma^2 - k^2\left(\Gamma - 1 + n^2\right) & -i\Gamma\gamma kn & i\Gamma k^2 n & 0 & 1 & 0 \\ i\Gamma\gamma kn & -\sigma^2 - k^2 n^2 & \Gamma\gamma k & -1 & 0 & 0 \\ -i\Gamma k^2 n & 0 & -2\sigma^2 - \Gamma k^2 n^2 & 0 & 0 & 0 \end{pmatrix}. \tag{10}$$

Solutions can only exist if the determinant of the matrix M is 0. This requirement generates the following dispersion relation for σ and n,
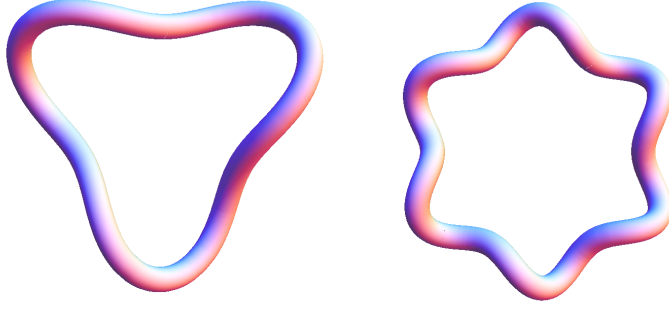
Figure 2: Some of the possible modes of equation 8. Pictured are $n = 3$ (left) and $n = 6$, however all modes of integer n are possible, with symmetry according to the value of n.

$$
\begin{aligned}
&- k^{10}n^6 \left(-1+n^2\right)^2 \Gamma \left(k^2 \left(-1+n^2\right) - \gamma^2\Gamma^2\right) \\
&- k^8 n^4 \left(-1+n^2\right) \left(k^2 \left(-1+n^2\right) \left(-2+\Gamma+2n^2(1+\Gamma)\right) + 2\Gamma \left(\gamma^2\Gamma + n^2 \left(1-\gamma^2\Gamma\right)\right)\right) \sigma^2 \\
&- k^4 n^2 \left(\left(1+n^2\right)\Gamma + k^2 \left(n^2(-4+\Gamma)+3\Gamma+2n^4(2+\Gamma)\right) + k^4 \left(-1+n^2\right)^2 \left(2(-1+\Gamma)+n^2(4+\Gamma)\right)\right)\sigma^4 \\
&- 2k^2 \left(1+n^2+k^4n^2\left(-1+n^2\right)^2 + k^2 \left(1-n^2+2n^4\right)\right)\sigma^6 = 0.
\end{aligned}
\tag{11}
$$

This equation is cubic in σ^2. A plot of σ^2 against n is shown in Fig. 1, which uses the values $k = 1$, $\gamma = 5$ and $\Gamma = 1$. This shows the possible values σ, which details the time evolution of the system, can take for each mode n. This is discussed further in the next section.

At this stage, it is possible to start to construct some of the solutions and generate some plots. The solution for σ is given by Eq. (11), and the values of the vector $\boldsymbol{x}$ by the the solution to $M \cdot \boldsymbol{x} = 0$. Thus $\boldsymbol{\alpha}^{(1)}$ is given by transforming $\boldsymbol{\beta}$ back to the original frame using the inverse of the original transformation given in Eq. (7),

$$
\boldsymbol{\alpha}^{(1)} = R_\gamma^{-1} . \left(\beta_1, \beta_2, \beta_3\right).
$$

The curve $x(s,t)$ can then be formed by integrating the first-order d_3,

$$
x(s,t) = \int d_3 \mathrm{d}s = x^{(0)}(s,t) + \int \left(\alpha_1^{(1)} d_2 - \alpha_2^{(1)} d_1\right) \mathrm{d}s.
$$

The general form of these modes is defined by their n value, and some of these plots are shown, for $n = 3$ and $n = 6$ in Fig. 2. The other modes follow this pattern; each mode has n-fold symmetry. Their evolution is detailed in the next section.

6 Time Evolution of Modes

The time evolution of the system is determined by the term $e^{\sigma t}$. The solutions fall into three classes, neutral modes with $\sigma = 0$, unstable modes with $\sigma > 0$, and stable modes with $\sigma < 0$. It is clear that all of these types of solutions are seen in the dispersion relation displayed in Fig. 1.
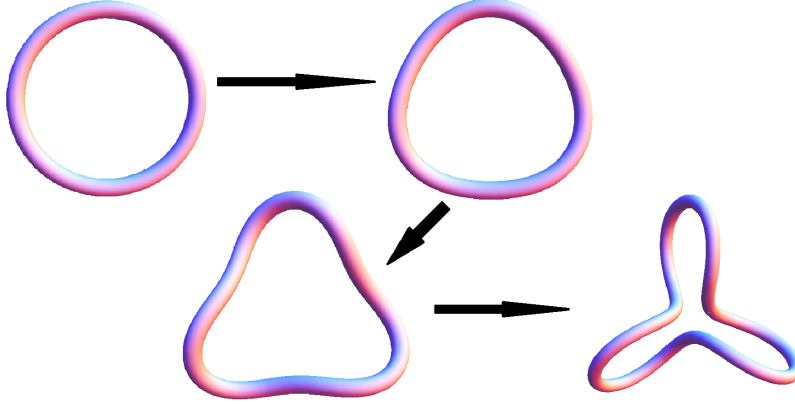
Figure 3: The time evolution of the mode $n = 3$. At times past the pertubative regime, the ring starts to touch at the centre as the images suggest. This shows the limited nature of the first-order solution.

Firstly, there are neutral modes at $n = 0, \pm 1$. The $n = 0$ being the entirely unperturbed solution, and $n = \pm 1$ being a planar ellipse shape. As these modes have $\sigma = 0$, they remain in this configuration for all time.

Secondly, there are unstable modes in the range $1 < n < n_c$, in this case $n = \pm 2, \pm 3, \pm 4, \pm 5$. If unstable modes exist, they dominate any real situation due to their ever increasing amplitudes. The fastest growing mode is the one with the greatest value of σ, which will dominate any real situation over long periods of time. This helps to explain why certain modes appear in numerical analysis [10]. Here, the fastest growing mode is somewhere around $n = 3$ ($n \approx 2.88$), so I examine the growth of this mode in Fig. 3. As time goes on, the solution starts to grow out of the perturbative regime, and become less valid. This clear in the figure as the ring starts to touch at the centre—an entirely unphysical phenomenon.

The stable solutions are far simpler. The red and black lines of the plot in Fig. 1 represent rotations in space of the modes displayed in Fig. 2, with the rotations being in clockwise and anti-clockwise directions. Alternatively, this could be viewed as a clockwise or anti-clockwise traveling wave. The other case ($n > n_c$ on the blue curve in Fig. 1) represents a stable oscillation in mode amplitude, the ring perpetually growing and shrinking whilst rotating in space. All n-values have 3 modes possible, the two rotations and either an unstable mode or an amplitude modulated rotation. This first-order model is only valid for small times, so it is not enough to fully explain the system. In the next section, I begin to address this problem by considering higher order solutions.

7 Higher Order Solutions

The second-order equation

$$\hat{L}_0 \cdot \boldsymbol{\beta}^{(2)} = H_1(\boldsymbol{\beta}^{(1)}) \tag{12}$$

is solved by considering $\boldsymbol{\beta}^{(1)}$ to be in a normal mode and finding the second-order perturbation to that mode. Taking $\boldsymbol{\beta}^{(1)}$ to be the same form as above, H_1 becomes a function of s and t, and Eq. (12) can be solved by considering a homogeneous and particular solution. Only the particular
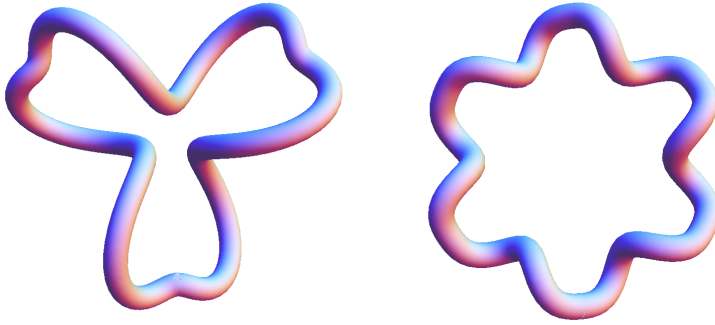
Figure 4: Plots of the modes $n = 3$ and $n = 6$ at second-order with the second-order term exaggerated, in order to show the deformation caused by the introduction of the second-order solution.

solution needs to be considered, as the homogeneous solution is exhibited at first-order, and hence can be cancelled out of the second-order solution by redefining the first-order amplitudes. The particular solution at second-order is of the form

$$\boldsymbol{\beta}^{(2)} = \boldsymbol{y} e^{2(\sigma t + ikns)}, \tag{13}$$

where $\boldsymbol{y}$ is determined by substituting Eq. (13) in Eq. (12). Hence, each mode n is partially composed of a smaller part of mode $2n$, which becomes more important at higher values of t, as the $2n$ mode grows at twice the rate of the mode n. This causes the plots in Figure 2 to become distorted, and would look like the plots in Figure 4. It should be noted, however, that these plots are unphysical as the second-order term has been magnified for visual effect.

At higher order, the system of equations in (9) are similarly reduced to

$$\hat{L}_0 \cdot \boldsymbol{\beta}^{(n)} = H_n(s, t), \tag{14}$$

which can be solved using the same method.

8   Conclusion

In this report I have introduced the Kirchhoff model, and described a perturbation scheme with which to analyse it. Under this scheme I looked at normal mode solutions, highlighting their n-fold symmetry. I considered the stability of these modes, looking at stable, neutral and unstable solutions. The unstable modes characterise much of the behaviour of the system seen in simulations [10], and plots such as Fig 1 pinpoint which modes will dominate the evolution. The first-order solution is limited, with the solutions growing unphysical quickly. This must be addressed by considering higher order solutions, which I have outlined how to obtain, and done so for second-order.

Whilst this accurately describes the appearance and evolution of individual modes, it does not describe their interaction. Now these modes are well defined, it is possible to approach a full nonlinear analysis of the problem. A solution can be considered a superposition of all of these possible modes. By considering the evolution of each modal amplitude to be dependent upon a far

9

slower time scale than the evolution of the ring, and requiring that amplitudes remains bounded, it is possible to obtain a set of equations describing the evolution of the amplitudes. These will take the form of a set of ODEs, the analysis of which will reveal how modes interact and evolve. This has been considered for a planar ring with only one unstable mode [6], and more thoroughly for straight rods [4, 7].

Acknowledgements

References

[1] B.D. Coleman, E.H. Dill, M. Lembo, Z. Lu, and I. Tobias. On the dynamics of rods in the theory of Kirchhoff and Clebsch. *Arch. Rational Mech. Anal. 121 339-359*, 1993.

[2] D.J.Struick. *Lectures on Classical Differential Geometry*. Dover Publications Inc., 1989.

[3] A. Goriely and M. Tabor. Nonlinear dynamics of filaments I. Dynamical instabilities. *Physica D 105 20-24*, 1997.

[4] A. Goriely and M Tabor. Nonlinear dynamics of filaments II. Nonlinear analysis. *Physica D 105 45-61*, 1997.

[5] A. Goriely and M. Tabor. Spontaneous helix hand reversal and tendril perversion in climbing plants. *Phys. Rev. Letters 80 no. 7*, 1998.

[6] A. Goriely, M. Tabor, and M. Nizette. The nonlinear dynamics of filaments. *Nonlinear Dyn. 21 101-133*, 2000.

[7] A. Goriely, M Tabor, and M. Nizette. On the nonlinear dynamics of elastic strips. *J. Nonlinear Sci. 11 3-45*, 2001.

[8] N.G. Hunt and J.E Hearst. Elastic model of DNA supercoiling in the infinite length limit. *J. Chem. Phys. 12 9329-9336*, 1991.

[9] J.E Keener. Knotted vortex filament in an ideal fluid. *J. Fluid Mech. 211 629-651*, 1990.

[10] I. Klapper. Biological applications of the dynamics of twisted elastic rods. *J. Comput. Phys. 125 325-337*, 1996.

[11] A. Mielke and P. Holmes. Spatially complex equilibria of buckled rods. *Arch. Ration. Mech. Analysis 101 319-348*, 1988.

[12] H.C. Spruit. Motion of magnetic flux tubes in the solar convection zone and chromosphere. *Astron. Astrophys. 98 155*, 1981.

[13] I. Tobias. A theory of thermal fluctuations in DNA miniplasmids. *Biophy. J. 74 2545-2553*, 1998.

[14] I. Tobias. Thermal fluctuations of small rings of intrinsically helical DNA treated like an elastic rod. *Phil. Trans. R. Soc. Lond. A 362 no. 1820 1387-1402*, 2004.

[15] G.H.M. van der Heijden, A.R. Champneys, and J.M.T. Thompson. The spatial complexity of localized buckling in rods with non-circular cross-section. *SIAM J. Appl. Math. 59 198-221*, 1981.

[16] H. Wada. A semiflexible polymer ring acting as a nano-propeller. *Eur. Phys. J. 28, 11-16*, 2009.

[17] J.P. Ward. *Solid Mechanics: An Introduction.* Springer, 1992.

[18] E.E. Zajac. Stability of two loop elasticas. *ASME 136-142*, 1962.